

Temperature Dependence of Structure and Morphology of Syndiotactic Polypropylene and Epitaxial Relationships with Isotactic Polypropylene

Andrew J. Lovinger* and Don D. Davis

AT&T Bell Laboratories, Murray Hill, New Jersey 07974

Bernard Lotz

Institut Charles Sadron (CRM-EAHP), CNRS-ULP, 6, rue Boussingault, Strasbourg, France

Received May 15, 1990

ABSTRACT: Structural investigation of syndiotactic polypropylene as a function of crystallization temperature revealed that at growth temperatures $\geq 105^\circ\text{C}$ this polymer crystallizes in the form of large, rectangular, single-crystal laths whose unit cell and interchain packing are in full agreement with our recently proposed alternative structural model. At lower temperatures of crystallization, an intermolecular packing disorder is progressively introduced along the *b* axis, which however does not affect packing in the *a* direction. The origin of this defect lies in kinetically driven incorporation of molecules of either chirality, whereas slow growth at the highest temperatures favors antichiral packing. At the same time, the morphology becomes axialitic and eventually spherulitic, although the tendency toward a rectangular lamellar habit is preserved. Within the syndiotactic polypropylene specimens, discrete populations of *isotactic* crystals were identified. This has important implications on the mechanism of syndiospecific polymerization and on the prevailing interpretation of stereoblock formation. The isotactic crystals grow as edge-on lamellae at the lateral sides of the syndiotactic laths through a specific epitaxial relationship discussed here. Because the heteroepitaxial match between isotactic and syndiotactic crystals is not as close as the homoepitaxial one within isotactic polypropylene, its crystals grow as stacks aligned parallel to the growth direction of the underlying syndiotactic laths.

Introduction

The past few years have seen a highly increased interest in the structure and morphology of stereoregular polypropylenes. This may at first seem surprising in view of the existence of isotactic and syndiotactic polypropylenes (iPP and sPP, respectively) for over 30 years following the pioneering synthetic and structural work of Natta and his colleagues (e.g., ref 1). For iPP, this work was followed by major and extensive morphological studies (e.g., refs 2-4). Nevertheless, some of the more detailed understanding of molecular-level processes in this polymer has occurred only very recently. This includes the establishment of unit-cell orientation and preferred growth direction in quadrites and spherulites of its dominant α phase,⁵ the elucidation of the molecular origin of lamellar branching in this polymorph,⁶ and the determination of the morphology⁷ and structure⁸ of the γ polymorph.

For syndiotactic polypropylene, research had been much less intense. In terms of crystal structure, the early work by Natta, Corradini, et al.^{1,9,10} had not been followed up for almost three decades. In terms of morphology, there was only one study (by Marchetti and Martuscelli¹¹); this dealt with solution-grown crystals. As a result, we became interested in the structural and morphological characteristics of this polymer. In our first work,¹² we examined melt-grown single crystals of sPP slowly cooled to ambient temperature and found a structure different from that adopted previously.^{1,9} The difference lay not in the molecular conformation (which is $(t_2g_2)_2$ as shown before^{1,9}) but in the interchain lattice and in the existence of packing defects. We then demonstrated¹³ the general validity of our alternative structure by removing any possible ambiguities arising from thin-film or epitaxial effects, thermal treatment or mechanical drawing, syndiotactic content, ordered-sequence length, molecular weight, or crystallinity and by finding unrecognized X-ray diffractometric support

for it even in previous studies.¹⁴⁻¹⁷ In the present work, we extend our structural investigation to the temperature dependence of the sPP molecular packing and especially to the variation of the lattice defects that we discovered previously¹² with temperature of crystallization.

As regards the morphology of sPP, the earlier work of Marchetti and Martuscelli¹¹ had found crystallization of single-crystal-like entities and aggregates from solution. These crystals had curved or irregular edges with no crystallographic faceting. Electron-diffraction analysis could not be performed because recording of well-defined diffraction patterns was not possible under the electron-irradiation conditions used.¹¹ In our present study we describe the results from a full morphological investigation of sPP crystallized from the melt over a wide range of temperatures.

The final aspect of this investigation concerns the mutual morphological and crystallographic relationships between the syndiotactic and isotactic isomers of polypropylene. Epitaxy of one polymer on crystals of another is extensively documented and has been demonstrated specifically for isotactic polypropylene in its binary blends with polyethylene¹⁸⁻²⁰ and polyamides.^{7,19,21} Here, we show that such epitaxial effects also exist between isotactic and syndiotactic polypropylene, and we use these to study not only the mutual relationships between these two isomers but also the chemical nature of polypropylene chains obtained through syndiospecific polymerization. The latter question has been the topic of much discussion, with most views favoring the formation of stereoblock polymers.^{14,17} As we will see, our results lead us to question this conclusion by demonstrating instead formation of separate populations of the two isomers.

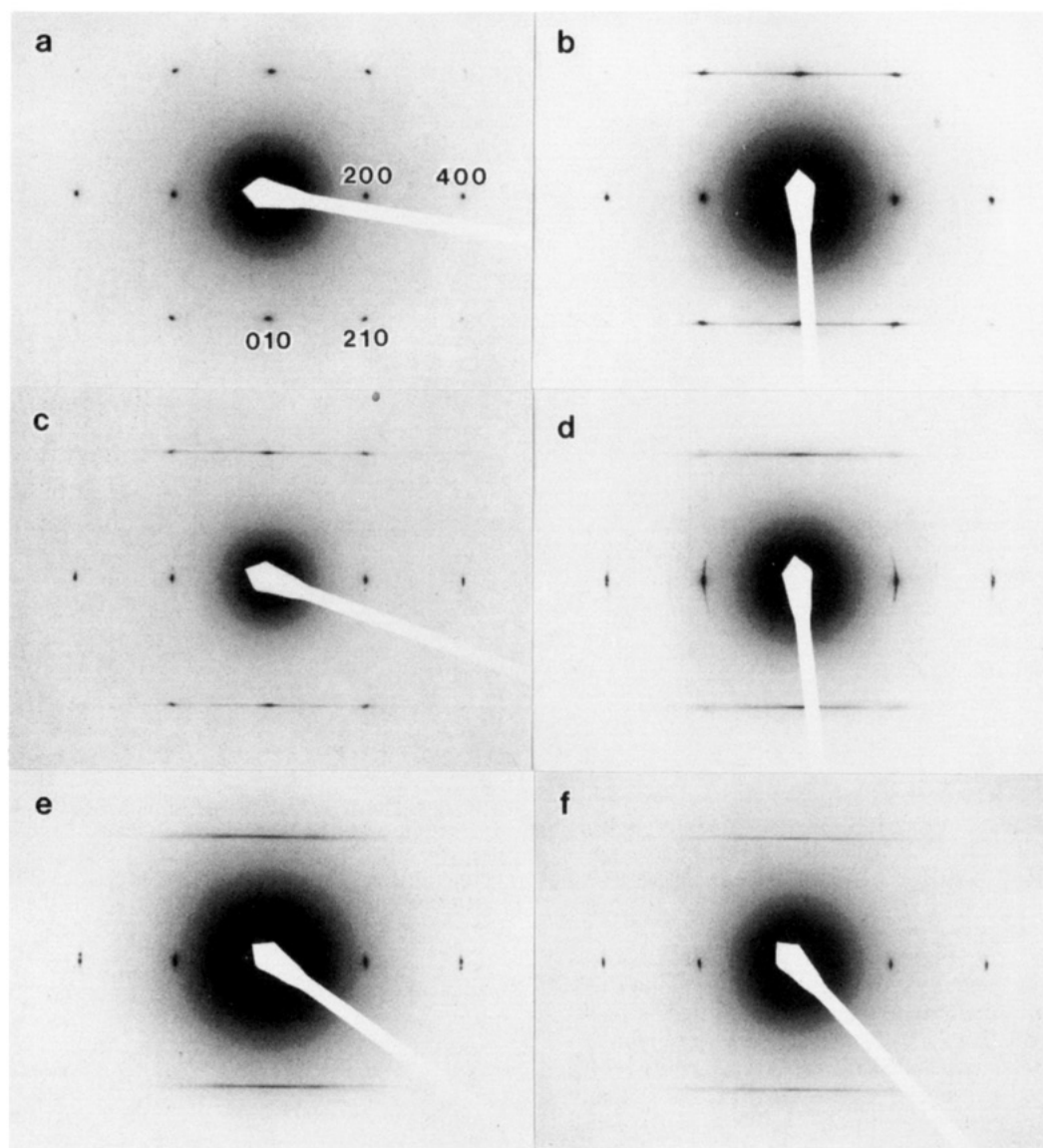


Figure 1. Electron-diffraction patterns from single crystals of syndiotactic polypropylene grown isothermally at (a) 105, (b) 100, (c) 90, (d) 80, (e) 70, and (f) 60 °C.

Experimental Section

The syndiotactic polypropylene used was the same as in our previous publications;^{12,13} its synthesis has been described in ref 12. It had a racemic diad content of 0.769 and syndiotactic and isotactic triad fractions of 0.698 and 0.159, respectively. We also used a sample kindly provided by Himont (Novara, Italy). Both specimens exhibited the same structural and morphological behavior.

Thin films (<50 nm) suitable for transmission electron microscopy and diffraction were prepared by casting from dilute solution in toluene or trichlorobenzene onto freshly cleaved mica. After evaporation of the solvent, the films were melted under dried nitrogen and heated to 150 °C to erase fully their previous morphologies (the actual melting temperature is 131–133 °C). They were then transferred rapidly into Mettler FP52 microscope ovens that were held at the desired crystallization temperatures (± 0.6 °C) and allowed to crystallize isothermally under dried nitrogen for appropriate periods of time. The samples were then rapidly cooled to ambient temperature, shadowed with platinum, coated with carbon, floated off the mica using distilled water, and deposited onto copper screening. After examination under phase-contrast optical microscopy, suitable areas were punched out and transferred to a JEOL 100-CX transmission electron microscope for further examination at 100 keV. Densitometric traces of the electron-diffraction patterns were recorded on a Bio-Rad video microdensitometer (Model 620) using a linear array detector.

Results and Discussion

(a) Structure. The crystalline structure of our specimens as a function of growth temperature was investigated using selected-area electron diffraction from single crystals. Such diffraction patterns are seen in Figure 1. The reflections are all of the $hk0$ type, implying that (since the crystals had not been tilted in the electron microscope) the molecular stems are parallel to the lamellar-thickness direction. The most notable feature of these diffraction patterns is the streak connecting the $h10$ reflections, whose intensity appears to increase with decreasing crystallization temperature. We had observed various and diverse manifestations of such a streak within each of our previous specimens,¹² which had been slowly cooled to room temperature. We can now explain this diversity by associating the extent of streaking with the temperature at which each crystal (or part of crystal) had been grown. It is also noteworthy that at the highest temperature studied (105 °C) the streaking is essentially fully absent and all reflections are sharp and well-defined.

The detailed features of the $h10$ reflections as a function of temperature and the very different behavior of their $h00$ counterparts can be clearly observed and compared through their densitometric traces (seen in Figures 2 and

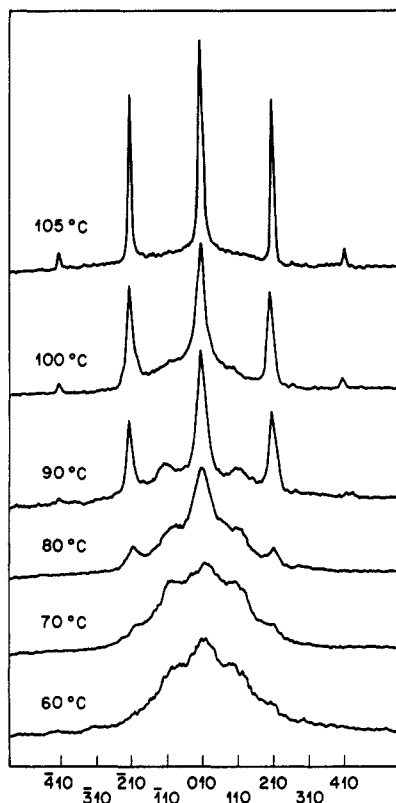


Figure 2. Densitometric traces through the $h10$ layer of electron-diffraction patterns from single crystals of syndiotactic polypropylene that had been grown isothermally at the indicated temperatures.

3, respectively). In Figure 2, the 105 °C trace shows persuasively the high crystallographic order of the (010) and (210) planes and the extremely small diffuse background that constitutes the streak. Very important in view of the alternative unit cells reported for sPP^{1,9,12,13} (to be discussed presently) is the *total* absence of any crystallographic scattering from the (110) and (310) planes at this crystallization temperature. At 100 °C, a distinct diffuse background can be seen, while the $h10$ reflections with h = even become weaker and broader. The trend continues at 90 °C, where now small but distinct diffuse maxima are seen at the 110 positions. At lower growth temperatures, crystallographic order is progressively lost, yet it is important to note that the resulting diffuse scattering remains maximized at the 010 position.

Contrary to these major changes in the $h10$ layer, the $h00$ reflections remain crystallographically sharp and intense throughout the entire range of crystallization temperatures (see Figure 3). The fact that no broadening trend exists at lower temperatures can be seen by extracting mean effective crystallite-size estimates from the 400 half-width using the Scherrer equation.²² As seen in the inset to Figure 3, these range between 25 and 29 nm for all temperatures (after instrumental correction). Of course, these values reflect the effects of crystal bending and radiation damage that are common during electron microscopy and should thus be viewed only comparatively; the original, undistorted dimensions are expected to be much greater.²³ The fact that the $h10$ reflections exhibit streaking while at the same time their $h00$ counterparts remain crystallographically sharp demonstrates the existence of a lattice defect along the b axis, which however does not affect packing in the a direction.

The operative defect is intimately related to the unit-cell structure of syndiotactic polypropylene, as we dis-

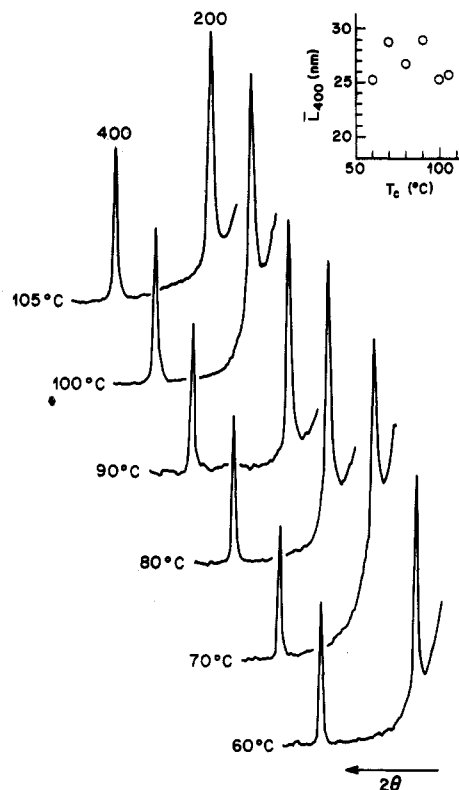


Figure 3. Densitometric traces through the $h00$ layer of electron-diffraction patterns from single crystals of syndiotactic polypropylene that had been grown isothermally at the indicated temperatures. The inset shows size estimates of the coherently scattering intermolecular crystalline regions that contribute to the 400 reflection.

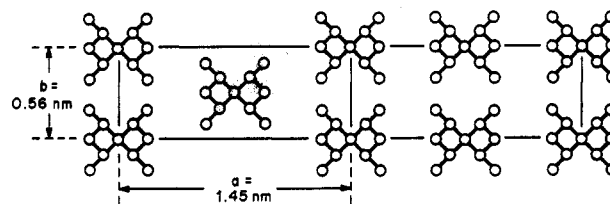


Figure 4. Possible intermolecular lattices for syndiotactic polypropylene in the dominant $(t_2g_2)_2$ conformation. The original^{1,9} C -centered unit cell is depicted in the left half, while our newly proposed^{12,13} alternative packing is shown in the right half.

cussed in our initial report¹² and as is summarized with the aid of Figure 4. Here, the left side denotes packing of sPP molecules in the C -centered unit cell proposed originally,^{1,9} while the right side depicts our alternative packing.^{12,13} In both cases the chain conformation is the same, i.e., $(t_2g_2)_2$, which is equivalent to a $4 \times 2/1$ helix in point-net notation, and the basic unit-cell dimensions are also the same. On the basis of our electron-diffraction results (Figures 1–3), we conclude that our newly proposed packing^{12,13} is adopted in a crystallographically regular manner at the highest crystallization temperatures (i.e., 105 °C or higher). At intermediate growth temperatures (i.e., down to ca. 80 °C), this unit cell is again adopted as the dominant structure, but with increasing disorder along b as temperature is lowered; the disorder consists of incorporation of chains in a C -centered fashion as in the left side of Figure 4, together with row vacancies (as discussed in our original publication).¹² At even lower temperatures (i.e., below ca. 80 °C) the existence of an almost continuous streak in place of crystallographically coherent scattering shows that this disordered packing along b predominates during crystal growth. We should note that in no case and at no growth temperature have

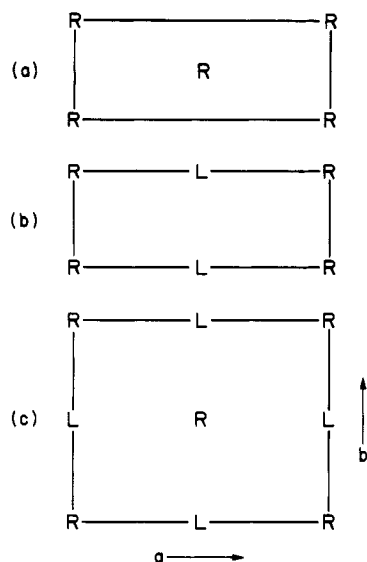


Figure 5. Chiral requirements for each of the proposed inter-chain lattices of syndiotactic polypropylene. (a) The original C-centered unit cell^{1,9} requires fully isochiral packing. (b, c) Our alternative structures^{12,13} are based upon antichiral packing either along the *a* axis only (b) or along both the *a* and *b* axes (c); the latter case results in doubling of the unit cell. R and L denote right- and left-handed molecular helices, respectively.

we observed a regular C-centered packing^{1,9} as depicted at the left of Figure 4.

The molecular origins of the different packing schemes lie in the handedness of the sPP helical chains as we demonstrated in ref 12 and as is seen schematically in Figure 5. For the original C-centered unit cell,^{1,9} steric reasons require that *all* chains be of the same hand (isochiral). For our alternative packing (Figure 5b) the molecules must be of opposite hand (antichiral) but *only* along *a* (i.e., on *ac* planes); along *b* there are no restrictions. While (for the sake of brevity) Figure 5b shows only helices of the same hand on the *bc* planes, packing could be (and most likely is) random. However, as we documented in ref 12 by use of electron diffraction on specimens tilted at various angles about the *a* and *b* axes, there is also evidence for irregular doubling of the unit cell in the *b* direction. Such doubling implies an *alternation* of helical handedness along *b* (see Figure 5c), rendering the chain packing antichiral in two dimensions.

These results also have clear implications on the lattice energetics in syndiotactic polypropylene as well as on the kinetics of crystallization. We infer that there must be an energetic gain in packing helices of opposite hand along *a* (and to a lesser extent along *b*) over incorporation of helices of the same hand. This should lead to preferential rejection of any isochiral molecules that may be preformed at the growth front. More likely, it should cause preferential adsorption and nucleation of molecules directly atop existing chains on the growth substrate (rather than in between them), accompanied by adoption of opposite helicity in a *template-like* manner. The fact that this regularity in packing is progressively reduced and eventually disappears as growth becomes faster (at lower temperatures) demonstrates the small energetic differences between the two types of chain packing and the increasingly dominant effects of *kinetic* factors.

(b) Morphology. We first examine the overall morphology of our syndiotactic polypropylene samples as a function of crystallization temperature using phase-contrast light microscopy. As seen in Figure 6, growth at temperatures from 60 to 105 °C yields a spectrum of

morphologies. At the highest temperature examined (Figure 6a), large, rectangular, and highly regular crystals are obtained, with lengths occasionally exceeding 100 μm (as in the upper right-hand corner of this figure). Individual crystals as well as aggregates nucleated heterogeneously (as seen at the lower left) are obtained with similar frequencies. Both are observed to contain multilayer overgrowths. As the temperature is lowered to 90 °C (Figure 6b), the morphology becomes axialitic. The lamellae are seen to fan out through screw dislocations at their edges, leading to incipient branching. At even lower temperatures, e.g., 70 °C (Figure 6c), branching is much more frequent and the morphology becomes fully spherulitic. With further cooling (Figure 6d), the only additional change is the expected large increase in nucleation density, leading to greatly reduced spherulitic sizes.

Greater morphological detail is attained by use of bright-field transmission electron microscopy. The tips of the large lathlike sPP crystals grown at 105 °C are seen in Figure 7a to be delineated by heavy irregular overgrowths. These are clearly rejected material, whose origin may be one of the following: (1) low-molecular-weight sPP that is fractionated during high-temperature growth and then crystallizes upon cooling;²⁴ (2) chemically disordered molecules, e.g., atactic or stereoblock, that cannot be incorporated into the sPP lattice; or (3) *isotactic* polypropylene molecules, whose presence in these samples we unambiguously demonstrate later in this paper. To identify the rejected species, we show in Figure 7b a higher magnification micrograph together with its electron-diffraction pattern. The bright-field image shows clearly that these species have an axialitic morphology, and the diffraction pattern identifies them uniquely with *syndiotactic* polypropylene (the 0.72-nm spacing is inconsistent with the structures of the α , β , or γ phases of isotactic polypropylene).

Morphological details as the crystallization temperature is lowered to 90 °C are seen in Figure 8. The overall growth habit is no longer that of a rectangular lath but exhibits fine-scale microfaceting with profuse screw dislocations and terraces. The fact that these dislocations are mostly localized at the periphery of the underlying lamella suggests that they originated primarily during rapid growth as the sample was cooled to room temperature. The very small irregular overgrowths seen at the borders reflect once again rejected species.

Crystallization at successively lower temperatures yields spherulitic structures, whose electron-microscopic appearance is typified in Figure 9 for a specimen crystallized at 70 °C. Stacks of lamellae are seen emanating from a central nucleus in Figure 9a; their underlying habit is still rectangular although quite distorted by profuse microfaceting (Figure 9b). This overall morphology is preserved at temperatures of crystallization as low as 60 °C. There are two unusual morphological features within these spherulites of syndiotactic polypropylene: (1) large areas of very high electron density (Figure 9a), which are consistent with development of a three-dimensional spherulitic microstructure by deviation of lamellae from the plane of the film; and (2) minute crystalline overgrowths near the edges of underlying lamellae and oriented transversely to them (Figure 9b).

Analysis of these two features shows that they are in fact related. The individual overgrowths can be seen at an early stage of their crystallization (Figure 10a) to be lamellae *on edge* that are nucleated precisely at the *lateral* growth facets of the sPP lamellae. They grow *transversely*, i.e., normal to the growth direction of the underlying sPP

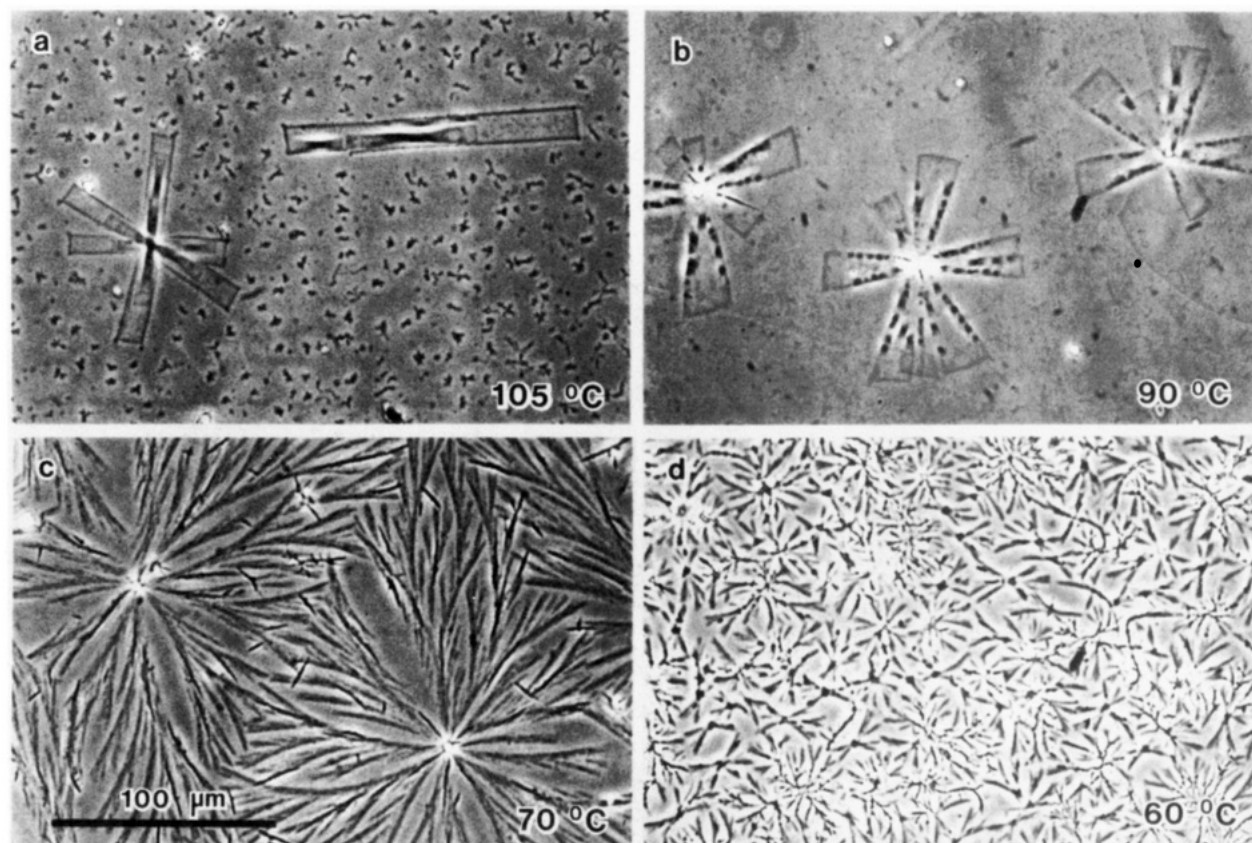


Figure 6. Phase-contrast optical micrographs of syndiotactic polypropylene crystallized isothermally at (a) 105 °C for 3 days, (b) 90 °C for 1 day, (c) 70 °C for 5 h, and (d) 60 °C for 1 h. At the end of their isothermal-crystallization treatments, the specimens were quickly cooled to ambient temperature. All micrographs are shown at the same magnification.

lamellae, and preferentially *outward*. This preferred outward direction implies that they are nucleated on growth steps, which indeed is energetically more facile. However, there are rare cases where growth is inward (e.g., arrowed crystal in Figure 10a). At this early stage of their growth, these edge-on crystals are seen to reach heights of up to 25 nm (the underlying flat-on lamellae are ca. 7 nm thick).

Turning now to the large, dense, radially directed regions of Figure 9a, we see at higher magnification (Figure 10b) that they, too, consist of lamellae on edge that are transversely disposed to the basal sPP crystals. However, these edge-on lamellae are now seen to be significantly higher, longer, and thicker than the individual ones of Figure 10a. Moreover, they are clearly *stacked parallel* to the preferred growth direction of the underlying sPP crystals (Figure 10b). These features imply that the edge-on stacks are in essence more fully developed versions of the individual edge-on lamellae. We proceed now with a crystallographic analysis of the edge-on population and of its relationship with the substrate.

(c) Epitaxy with Isotactic Polypropylene. Identification of the edge-on lamellae was made by using electron diffraction from areas such as the one circumscribed in Figure 10b. However, because the stacks generally grow with their long axes parallel to the preferred growth direction of the underlying lamellae, the composite diffraction patterns are not unambiguous. For this reason, we show in Figure 11 electron-diffraction evidence from one of the rare regions where these two populations have grown in a nonaligned manner. The flat-on lamellae yield reflections of syndiotactic polypropylene (identified with an s subscript) in the expected orientation. However, the edge-on crystals produce reflections that are *inconsistent*

with the syndiotactic isomer, but which we could ascribe to the dominant α phase of its *isotactic* counterpart (these are denoted by an i subscript in Figure 11b).

The isotactic polypropylene (iPP) is present within samples synthesized by syndiospecific catalysts should no longer be surprising, because we have recently¹³ demonstrated its existence within a number of sPP samples that had been studied earlier. Also, in a previous study²⁵ the presence of traces of sPP in isotactic polypropylene had been suspected. However, this is the first time that *individual* iPP crystals could be identified (and examined) as a separate population within sPP specimens. It is clear from Figures 10a and 11a that their morphology is different from any described previously for the α phase of isotactic polypropylene.²⁻⁶ However, as is described below, this morphology is closely related to the typical ones of iPP, i.e., (1) flat rectangular laths growing along their a^* crystallographic axis, with the b axis transverse, and (2) cross-hatched assemblies ("quadrites") of edge-on lamellae joined along their b axes through homoepitaxy of their a and c axes.

The diffraction pattern of Figure 11b shows that the b crystallographic axes of the iPP lamellae are parallel to the substrate and lie transversely to the growth direction of their stack. Thus, these edge-on lamellae could constitute one of the two populations of a quadrite, in which the second component would consist of flat-on lamellae growing along the stack axis. There is some morphological evidence for that. Figure 10b shows *within* the stack of edge-on lamellae numerous striations running lengthwise along its growth direction. These could be edges of flat-on lamellae that are partly obscured by overgrowths of edge-on crystals produced by the well-known homoepitaxy.²⁻⁶ The overall morphology would then be as the

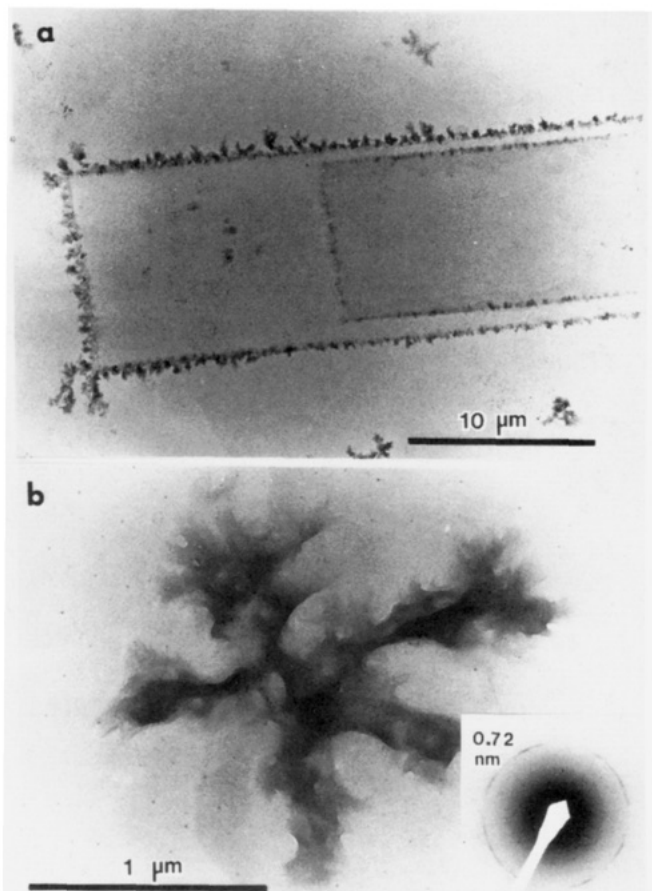


Figure 7. (a) Transmission electron micrograph of the tip of single crystals of syndiotactic polypropylene crystallized isothermally at 105 °C for 3 days. (b) Higher magnification of one of the small spherulitic entities at the border of the large lamella in (a), together with its electron-diffraction pattern.

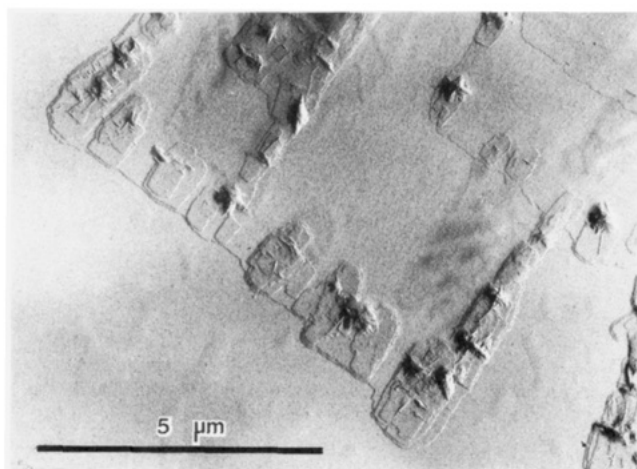


Figure 8. Tips of syndiotactic polypropylene spherulites crystallized at 90 °C for 1 day, recorded by bright-field transmission electron microscopy.

one depicted schematically in Figure 12, where edge-on lamellae of iPP (nucleated by sPP substrate crystals) would in turn nucleate growth of flat-on iPP lamellae in a homoepitaxial relationship. Crystallographic support for this scheme lies in the presence of the 110 reflections of isotactic polypropylene in Figure 11b. These reflections can arise only from flat-on iPP lamellae, for which the 110 planes are in the reflecting position, as is usual in single-crystal electron-diffraction patterns.

So far we have shown that the stacks are iPP quadrites grown on sPP crystals in the manner depicted in Figure

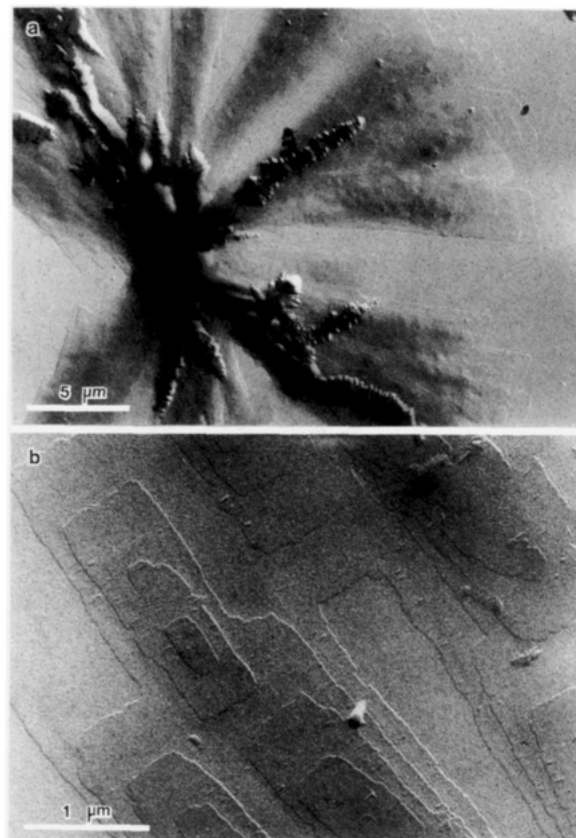


Figure 9. (a) Electron microscopic appearance of a syndiotactic polypropylene spherulite crystallized isothermally at 70 °C for 5 h. (b) Detail of lamellar morphology at higher magnification.

12. But what causes their initial nucleation in the first place? The crystallographic arrangements between the two isomers observed in composite electron-diffraction patterns suggest a specific form of epitaxy, which we show schematically in Figure 13. Here, the underlying sPP molecules are depicted with dashed lines in an *a*-axis projection. As in our previous papers,^{12,13} we show here only the *top* surface of the molecules on the *bc* planes, which will serve as the substrate for growth on the lateral surfaces of the sPP lamella. We should recall^{12,13} that these top surfaces consist of rows of $\{\text{CH}_3, \text{CH}_2, \text{CH}_3\}$ groups that are inclined at $\sim 45^\circ$ to the molecular axes in the same or opposite sense according to the type of sPP chain packing (i.e., as in parts a and b of Figure 13, respectively).

As regards iPP, its molecules adopt a 3/1-helical conformation, which is shown in Figure 13 by heavy solid lines. The *bottom* surface of these helices (i.e., the one that will be in contact with the top surface of the sPP chains) consists of CH_3 groups, which are shown shaded in Figure 13. As has been discussed extensively,^{6,19} these methyl groups are arranged in closely packed planes along the two diagonals of the monoclinic unit cell of the α phase of iPP (i.e., on the (101) and (10 $\bar{1}$) planes). We can see in Figure 13a that these closely packed rows of methyl groups of iPP can be aligned parallel to the 45° rows of the sPP substrate in a sterically reasonable manner. The same holds true for the doubled unit cell of sPP (Figure 13b), where the underlying rows alternate at $\pm 45^\circ$ to the molecular direction. These mutual crystallographic relationships between iPP and sPP could provide the epitaxial driving force for initiation of iPP branches at the sides of sPP lamellae in the manner depicted schematically in Figure 12 on the basis of our electron-diffraction results.

However, a third mutual arrangement is also possible, since iPP molecules could be deposited *parallel* to their

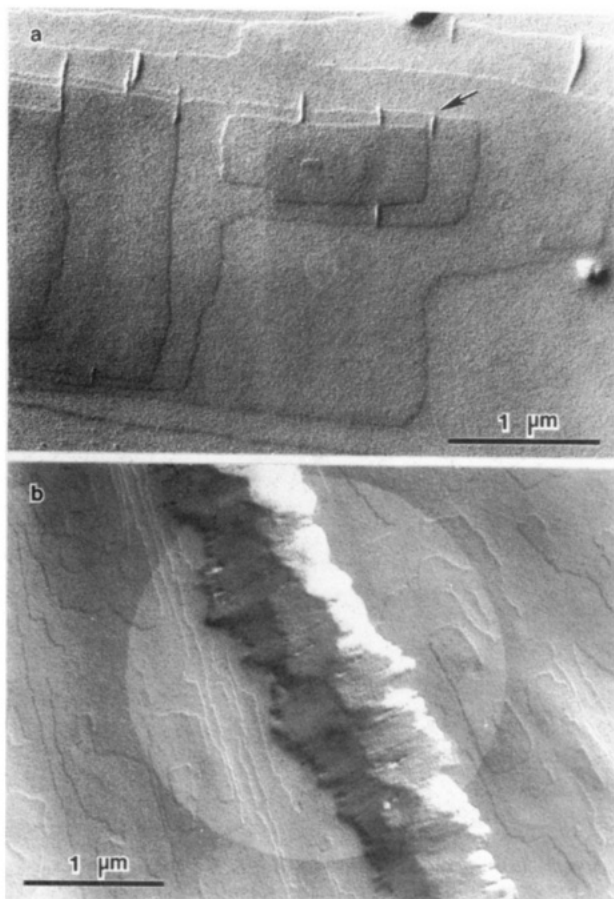


Figure 10. Details of transversely oriented crystalline overgrowths on lamellae of syndiotactic polypropylene grown at 70 °C: (a) individual overgrowths; (b) stacked overgrowths, radially oriented. The circular region in (b) delineates an area selected for electron diffraction.

sPP counterparts while keeping essentially the same methyl contacts as in Figure 13a,b. This parallel packing is seen schematically in Figure 13c (to conserve space, a parallel packing on an sPP substrate such as that of Figure 13b is not shown). This alternative deposition would cause the initial iPP growth to be a *flat-on* lamella, from which the edge-on stacks could subsequently emanate through the usual homoepitaxy. While this nucleation scheme is possible, we have only rarely observed any edges of flat-on iPP lamellae protruding at the leading or lateral sides of these stacks.

It is clear from Figure 13 that, despite the mutual alignment of the densely packed rows of iPP and sPP, the epitaxial match is not very close. For example, the lengths of the *a* and *c* axes of iPP correspond to only 89.86% and 87.84% (respectively) of the length of the *c* axis of sPP. These mismatches may explain the infrequent occurrence of iPP initiation on sPP, as seen for example in Figures 9b and 10a. They may also explain the formation of profuse lamellar stacks of iPP, since the homoepitaxial branching within this polymer has a negligibly small mismatch ($a = 0.665$ nm, $c = 0.650$ nm) compared to the heteroepitaxial initiation of iPP on sPP.

In order to test independently the validity of our proposed epitaxial iPP/sPP relationship, we designed a specific experiment utilizing epitaxial crystallization of sPP on single crystals of an organic substrate (*p*-terphenyl). The sPP contact plane in this case was found to be the *bc* plane. After removal of the *p*-terphenyl by dissolution in chloroform, this plane was used as a substrate for condensation-crystallization of iPP vapors, following

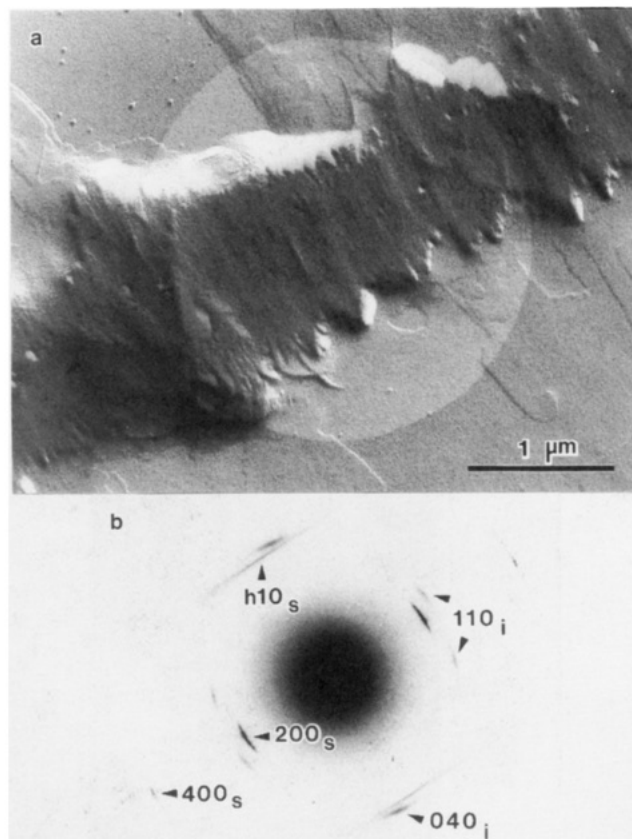


Figure 11. (a) Region where the edge-on and flat-on lamellae have grown in a nonparallel orientation and (b) its electron-diffraction pattern from the circular area delineated in (a) (shown in correct mutual orientation). Subscripts *s* and *i* denote syndiotactic and isotactic polypropylene, respectively.

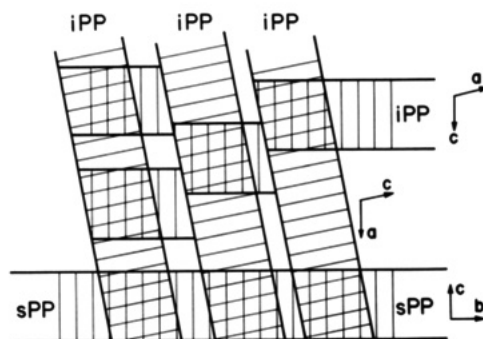


Figure 12. Schematic drawing of the growth of α -phase isotactic polypropylene quadrites on flat-on crystals of syndiotactic polypropylene. Edge-on lamellae of iPP are nucleated on sPP crystals and, in turn, nucleate growth of flat-on iPP lamellae through homoepitaxy of their *a* and *c* axes.

a technique already used to establish the iPP/polyamide relationship.¹⁹ The resulting electron-diffraction pattern is seen in Figure 14.

This pattern demonstrates that the *c* axis of iPP is approximately normal to the *c* axis of sPP. Presence of the 110 and 130 reflections of iPP (as well as of the outer reflections) indicates a quadritic structure with preferred orientation of the chains as indicated in Figure 13a,b. The large angular spread of the *hk0* reflections of iPP in Figure 14 follows naturally from the nonorthogonal orientation of the *c* axes of iPP and sPP, when the two possible (symmetrical) dispositions of the iPP lattice on the sPP substrate are considered. Figure 14 therefore provides complementary and independent support for our model of interaction of iPP and sPP lattices presented in Figures 12 and 13.

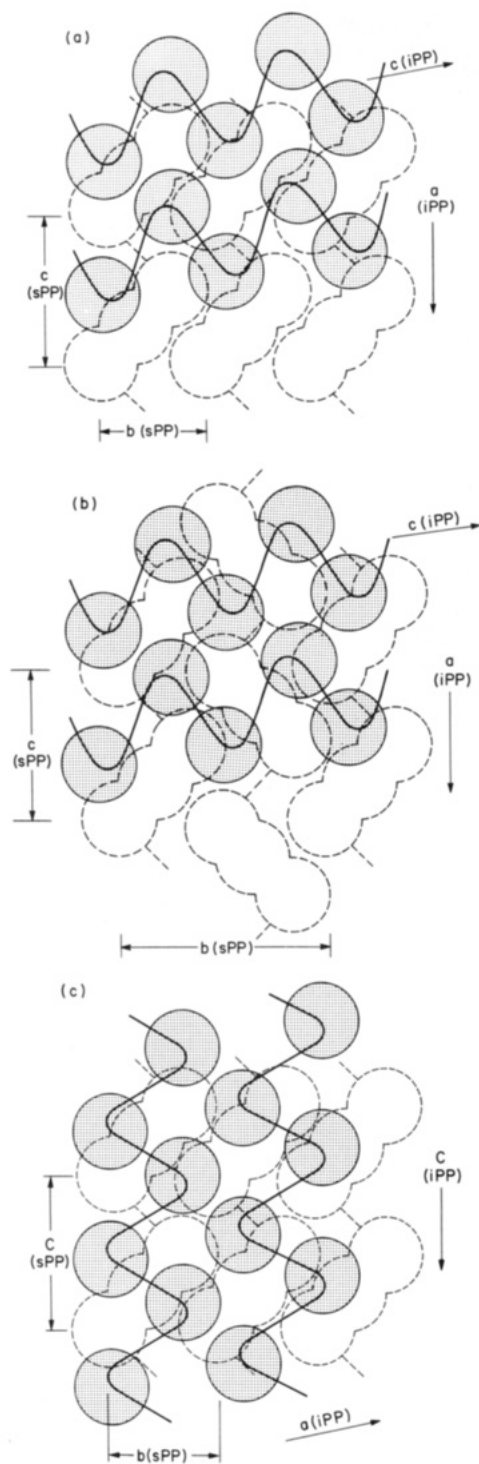


Figure 13. Possible epitaxial relationships between isotactic and syndiotactic polypropylene leading to branching as in Figure 12 for the two types of sPP unit cell: (a) simple unit cell as in Figure 5a,b; (b) doubled unit cell as in Figure 5c. The dashed lines denote the underlying sPP molecules, while the solid lines correspond to the depositing iPP chains. (c) A third possible epitaxial arrangement involving *parallel* isotactic and syndiotactic chains, which would cause growth of *flat-on* lamellae as the initial constituents of iPP quadrites.

Conclusions

We have shown that the structure and morphology of syndiotactic polypropylene depend very sensitively and in a unique manner on the temperature of crystallization. At the highest temperatures, very large rectangular laths are grown from the melt, whose crystallographic structure is in full agreement with our newly proposed unit cell. As the temperature of crystallization is lowered, kinetic factors

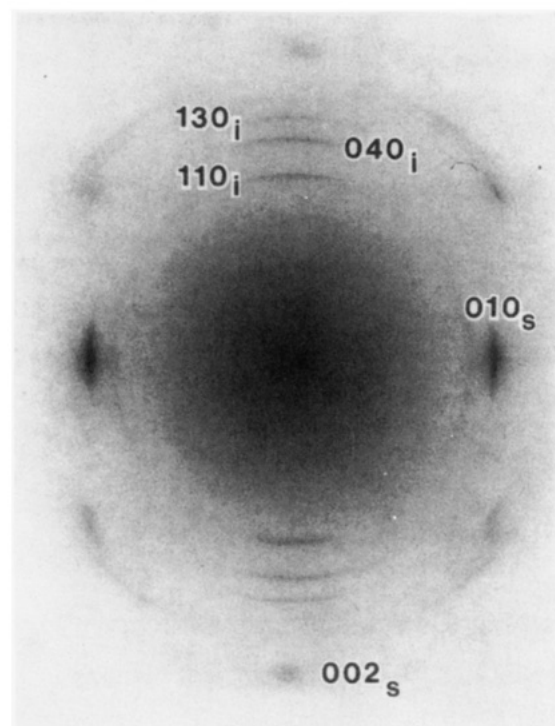


Figure 14. Composite electron-diffraction pattern showing epitaxial relationships between isotactic polypropylene vacuum-evaporated onto the *bc* facets of syndiotactic polypropylene. The latter facet had been obtained by epitaxial crystallization of sPP on *p*-terphenyl.

favor the progressive introduction of a packing disorder along the *b* axis of the unit cell, while the morphology becomes more typically axialitic and eventually spherulitic. Additionally, lamellae appear on edge transversely to the underlying flat-on laths. We demonstrated by electron diffraction that these edge-on crystals are of the α phase of *isotactic* polypropylene and are initiated by a specific epitaxial relationship with the lateral surfaces of the sPP lamellae. This heteroepitaxial match is not very close, a fact that may explain the infrequent initiation of these edge-on iPP crystals. However, because of the tendency of iPP toward quadritic branching through homoepitaxy, these iPP lamellae proliferate by formation of stacks in the radial direction of their underlying sPP spherulites. The fact that separate iPP entities are morphologically and crystallographically identified within sPP samples confirms our previous conclusion that syndiospecific polymerization produces separate syndiotactic polypropylene molecules together with a minority population of isotactic chains, rather than (or in addition to) stereoblock molecules.

Acknowledgment. We are grateful to Dr. R. E. Cais and to Himont (Novara, Italy) for synthesis of the syndiotactic polypropylene samples used in this study.

References and Notes

- (1) Natta, G.; Pasquon, I.; Corradini, P.; Peraldo, M.; Pegoraro, M.; Zambelli, A. *Rend. Acc. Naz. Lincei* **1960**, *28*, 539.
- (2) Khoury, F. J. *Res. Natl. Bur. Std.* **1966**, *70A*, 29.
- (3) Padden, F. J.; Keith, H. D. *J. Appl. Phys.* **1966**, *37*, 4013.
- (4) Padden, F. J.; Keith, H. D. *J. Appl. Phys.* **1973**, *44*, 1217.
- (5) Lovinger, A. J. *J. Polym. Sci., Polym. Phys. Ed.* **1983**, *21*, 97.
- (6) Lotz, B.; Wittmann, J. C. *J. Polym. Sci., Polym. Phys. Ed.* **1986**, *24*, 1541.
- (7) Lotz, B.; Graff, S.; Wittmann, J. C. *J. Polym. Sci., Polym. Phys. Ed.* **1986**, *24*, 2017.
- (8) Brückner, S.; Meille, S. V. *Nature* **1989**, *340*, 455.

- (9) Corradini, P.; Natta, G.; Ganis, P.; Temussi, P. A. *J. Polym. Sci., Part C* **1967**, *16*, 2477.
- (10) Natta, G.; Peraldo, A.; Allegra, G. *Makromol. Chem.* **1964**, *75*, 215.
- (11) Marchetti, A.; Martuscelli, E. *J. Polym. Sci., Polym. Phys. Ed.* **1974**, *12*, 1649.
- (12) Lotz, B.; Lovinger, A. J.; Cais, R. E. *Macromolecules* **1988**, *21*, 2375.
- (13) Lovinger, A. J.; Lotz, B.; Davis, D. D. *Polymer* **1990**, *31*, 2253.
- (14) Natta, G.; Pasquon, I.; Zambelli, A. *J. Am. Chem. Soc.* **1962**, *84*, 1488.
- (15) Zambelli, A.; Natta, G.; Pasquon, I. *J. Polym. Sci., Part C* **1963**, *4*, 411.
- (16) Inagaki, H.; Miyamoto, T.; Ohta, S. *J. Phys. Chem.* **1966**, *70*, 3420.
- (17) Ogawa, T.; Elias, H.-G. *J. Macromol. Sci., Chem.* **1982**, *A17*, 727.
- (18) Gross, B.; Petermann, J. *J. Mater. Sci.* **1984**, *19*, 105.
- (19) Lotz, B.; Wittmann, J. C. *J. Polym. Sci., Polym. Phys. Ed.* **1986**, *24*, 1559.
- (20) Lotz, B.; Wittmann, J. C. *J. Polym. Sci., Polym. Phys. Ed.* **1987**, *25*, 1079.
- (21) Seth, K. K.; Kempster, C. J. E. *J. Polym. Sci., Polym. Symp.* **1977**, *58*, 297.
- (22) Scherrer, P. *Göttingen Nachr.* **1918**, *2*, 98.
- (23) Thomas, E. L.; Sass, S. L.; Kramer, E. J. *J. Polym. Sci., Polym. Phys. Ed.* **1974**, *12*, 1015.
- (24) Keith, H. D.; Padden, F. J., Jr. *J. Appl. Phys.* **1964**, *35*, 1270, 1286.
- (25) Addink, E. J.; Beintema, J. *Polymer* **1961**, *2*, 165.

Registry No. s-PP, 26063-22-9; i-PP, 25085-53-4.